



: SPIO
 가 ,
 가
 : SPIO 27
 49 , 38-71 (56)
 21 , 가 6 87가
 SPIO T2 -, proton-density
 - (Conventional Spin Echo; CSE) (Turbo Spin
 Echo; TSE) , T1 - (Fast low-
 angle shot, T1wFLASH), Fourier (half-Fourier-acquisition single-shot-TSE,
 HASTE), T2*- (fast imaging with steady state
 precession, T2*wFISP), T2 - (Breath-hold -TSE,
 T2wBHTSE) ,
 (Signal to Noise ratio,
 S/N) (Percentage of signal
 intensity loss, PSIL) , (Contrast to Noise
 ratio, C/N) (Image artifact)
 (Lesion conspicuity) .
 : S/N
 S/N
 . PSIL T2*wFISP 가
 (P < 0.05). T2 CSE T2*wFISP PSIL
 T2 TSE (P < 0.05). C/N T2*wFISP
 가 (P < 0.05), T2-TSE HASTE T2*wFISP C/N
 T2*wFISP
 (P< 0.05). (sensitivity)
 T1wFLASH 가
 T2*wFISP T2wTSE 가
 : SPIO
 T2*wFISP 가
 TSE T1 FLASH 가

1
2
3

8가 MR
 가
 (Lesion conspicuity)
 (Image artifact)
 가 가(unacceptable, 1), (poor, 2),
 (fair, 3), (good, 4) (excellent, 5)
 Wilcoxon signed ranks test
 (p < 0.05).
 3cm , 3cm
 5cm, 5cm
 가 가
 paired student t-test
 (p < 0.05).

Table 1. Quantitative Analysis: Effect of SPIO Enhancement on S/Ns in 27 Patients with Hepatocellular Carcinoma

MR Pulse Sequence	Tumor S/N	Liver S/N [†]
T2wSE		
precontrast	7.08 ± 4.73	4.42 ± 2.52
postcontrast	7.42 ± 5.36	1.90 ± 0.84
PDwSE		
precontrast	10.21 ± 7.41	9.00 ± 5.31
postcontrast	12.03 ± 6.12	6.37 ± 3.44
T2wTSE		
precontrast	8.63 ± 4.26	6.00 ± 2.57
postcontrast	9.28 ± 5.37	3.45 ± 1.99
PDwTSE		
precontrast	15.57 ± 14.46	13.46 ± 10.26
postcontrast	14.13 ± 8.63	8.51 ± 4.67
T1wFLASH		
precontrast	11.90 ± 4.76	14.29 ± 5.40
postcontrast	12.81 ± 5.81	9.33 ± 3.88
HASTE		
precontrast	13.78 ± 5.70	10.27 ± 3.71
postcontrast	13.03 ± 4.79	6.44 ± 2.77
T2*wFISP		
precontrast	13.02 ± 5.90	11.66 ± 5.30
postcontrast	16.19 ± 7.86*	3.66 ± 2.34
T2wBHTSE		
precontrast	7.14 ± 2.65	4.48 ± 1.40
postcontrast	6.01 ± 3.23	2.15 ± 0.77

Note - Numbers are mean ± standard deviation.
 * - Mean tumor S/N of postcontrast image was higher (p < .05) than that of precontrast image in T2*wFISP sequence.
 In other sequence images, There are no significant differences (p > .05) in tumor S/Ns between pre- and postcontrast images.
 † - Every mean S/Ns of postcontrast image was lower (p < .05) than those of precontrast image of liver.

SPIO
 S/N
 (Table 1, Fig. 1). SPIO
 S/N
 S/N
 가 27 PSIL
 T2*wFISP 66.7% 가
 T2wSE T2wTSE
 54.7% 43.7% PSIL

Table 2. Quantitative Analysis: Percentage of Signal Loss Intensity of Liver Parenchyme in 27 Liver Cirrhosis Patients

MR Pulse Sequence	PSIL *	Rank
Non-Breath hold sequence		
T2wSE	54.71 ± 17.28	2 [†]
PDwSE	30.97 ± 18.16	6
T2wTSE	43.66 ± 18.05	3 [†]
PDwTSE	29.05 ± 15.94	7
Breath hold sequence		
T1wFLASH	19.44 ± 18.88	8
HASTE	35.52 ± 19.31	5
T2*wFISP	66.69 ± 16.26	1 [†]
T2wBHTSE	42.34 ± 13.08	4

Note - Numbers are mean ± standard deviation.
 * - PSIL means percentage of signal loss intensity of liver.
 = [(SI enhanced - SI unenhanced) / SI unenhanced] × 100
 † - The PSIL of T2*wFISP image is the highest of others images.
 ‡ - These two images have higher PSIL than other images significantly (p < .05) except T2*wFISP.

Table 3. Quantitative Analysis: Lesion-to-Liver Contrast-to-Noise Ratio of Hepatocellular Carcinoma

MR Pulse Sequence	Precontrast Image		Postcontrast Image	
	C/N	Rank	C/N	Rank
Non-Breath hold sequence				
T2wSE	2.65 ± 3.11	3	5.51 ± 4.96	6
PDwSE	1.21 ± 2.59	7	5.65 ± 4.94	5
T2wTSE	2.62 ± 2.29	4	5.82 ± 4.20	3
PDwTSE	2.10 ± 5.11	5	5.82 ± 4.52	4
Breath hold sequence				
T1wFLASH	2.40 ± 3.78	8	3.38 ± 2.79	8
HASTE	3.51 ± 3.18	1	6.59 ± 3.66	2
T2*wFISP	1.36 ± 2.67	6	12.53 ± 6.61	1*
T2wBHTSE	2.66 ± 1.96	2	3.85 ± 2.83	7

Note - Datas are given as mean ± standard deviation.
 * - The C/N of T2*wFISP image is highest of other images (p < .05).

($p < 0.05$) (Table 2, Fig. 1).
 가 T2*wFISP T2wTSE 가 T2wBHTSE T2wSE, . 3cm
 가 C/N (p < 0.05), HASTE T2wTSE 가 (94%). T2*wFISP
 가 C/N (Table 3). T1w-FLASH PDwTSE PDwSE T2wSE,
 가 , 가 (p < 0.05).
 T2*wFISP (Table 4, Fig. 2). 가 가 (1-2).
 T1wFLASH 가 3 cm 가 (3-4).
 가 (Table 5). SPIO (reticuloendothelial system) SPIO

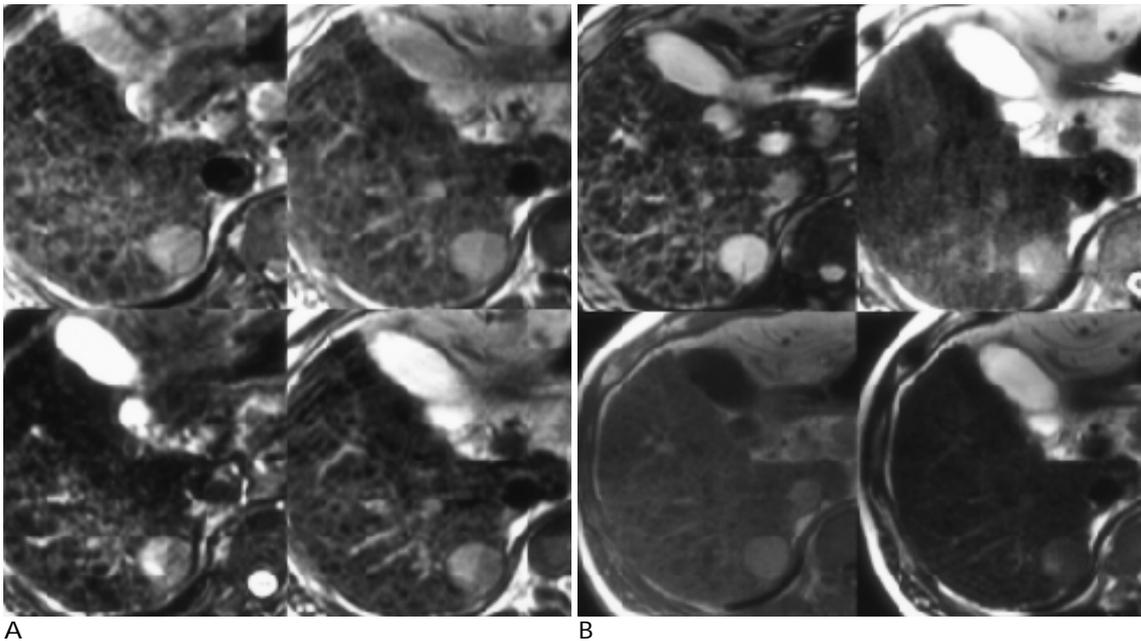


Fig. 2. Postcontrast images of 45-year-old man with a hepatocellular carcinoma in segment 6. This patient had severe degree of liver cirrhosis (child class C)
 A. Non-breath-hold images with SE and TSE MR technique.
 Top left: PDwSE image. Bottom left: T2wSE image. Top right: PDwTSE image. Bottom right: T2wTSE image.
 B. Breath-hold images. Top left: T2*wFISP image. Bottom left: T1wFLASH image. Top right: HASTE image. Bottom right: T2wBHTSE image.
 A tumor in segment 6 is depicted more conspicuous in four non-breath-hold images (A) and breath-hold T2*wFISP image (top left in B) than other non-breath-hold images. The lesion-to-liver contrast is worst in the T2wBHTSE image (bottom right in B). The normal hepatic anatomy is not seen as well on the HASTE image (top right in B) because of increased inherent blurring.

refocusing (16). pulse가

T2* sequence long TE (8). T1 Flip angle , PSIL SE가 TSE TSE 180 re- (20-21). focusing pulse (16). SPIO가 , HASTE

T2wBHTSE C/N T1wFLASH 가 T2*wFISP 가 cho-train length e- (TR/TE=300/15) 가 Gradient echo T2* -weighted sequence 가 SPIO (inherent blurring) 가 TSE가 가

Schwarz (16) SPIO SE TSE lesion to liver C/N SE Stark (22) T2wTSE SE SE가 TSE 0.6T T1, T2 가 Bellin (14) 1.5T 가 가 Yamamoto (23) 1.5T SE 가 TSE C/N FLASH (50/10, flip angle 40 degree) 가 가 (hypointense rim)가 SPIO 가 (24). SPIO 가 가 가 T1wFLASH 3cm 가 TSE SE Elizondo (25) SPIO 가 가 가 C/N , 4가 gradient echo T2*wFISP Yamamoto (23) Clemento (26) HASTE가 SPIO T2*wFISP 가 T2*wFISP 가 가

		FISP	T2wTSE	가	SPIO	MR
가	3cm		가	가		
conspicuity			C/N		T1wFLASH,	T2wTSE
			le-		T1wFLASH, T2*wFISP,	T2w TSE
		T2*wFISP		가		
가	가	SPIO	T2			
	가		T2*wFISP			
	가		가			
	8가	spin echo	C/N			
		가	SPIO	MR		
				T2		
가			C/N			
	TSE	SE	TSE			
SPIO	가	T2	TSE			
		가	가			
				SPIO		
	T2	가	T2			
Gradin (27)	가					
	Poekler-Schoeniger (28)					
T1wFLASH	PSIL	가	lesion to liver contrast			
	가			SPIO	MR	
	가					
SPIO	T1			SPIO	T2	
					T2	
					T1wFLASH	
가	Grangier (29)					
SPIO	T1wFLASH	T1				
					T1wFLASH	

- Liu CL, Fan ST. Nonresectional therapies for hepatocellular carcinoma. *Am J Surg* 1997;173:358-365
- Farmer DG, Rosove MH, Shaked A, Busuttill RW. Current treatment modalities for hepatocellular carcinoma. *Ann Surg* 1994;219:236-247
- Brasch RC. New directions in the development of MR imaging contrast media. *Radiology* 1992;183:1-11
- Van Beers BE. Contrast-enhanced MR imaginag of the liver. *Radiology* 1997;203:297-306
- Weissleder R, Stark DD, Engelstad BL, et al. Superparamagnetic iron oxide: pharmacokinetics and toxicity. *AJR Am J Roentgenol* 1989;152:167-173
- Hahn PF and Saini S. Liver-specific MR imaging contrast agents. *Radiol Clin North Am* 1998;36:287-297
- Petersein J, Saini S, and Weissleder R. Liver II: iron oxide-based reticuloendothelial contrast agents for MR imaging. *Radiol Clin North Am* 1996;4:53-60
- Fret CJ, Elizondo G, Weissleder R, et al. Superparamagnetic iron oxide-enhanced MR imaging: pulse sequence optimization for detection of liver cancer. *Radiology* 1989;172:393-397
- Tsang YM, Stark DD, et al. Hepatic micrometastasis in the rat : Ferrite-enhanced MR imaging. *Radiology* 1988;167:21-24
- Saini S, Stark DD, et al. Ferrite particles: a superparamagnetic MR contrast agent for enhanced detection of liver carcinoma. *Radiology* 1987;162:217-222
- Frets CJ, Strak DD, et al. Detection of hepatic metastases: comparison of contrast-enhanced CT, unenhanced MR imaging, and iron oxide-enhanced MR imaging. *AJR Am J Roentgenol* 1990;155:763-770
- Winter TC III, Freeny PC, Nighiem HV, et al. MR imaging with IV superparamagnetic iron oxide: efficacy in the detection of focal hepatic lesions. *AJR Am J Roentgenol* 1993;161:1191-1198
- Yamamoto H, Yasuyuki Y, et al. Hepatocellular carcinoma in cirrhotic livers: detection with unenhanced and iron oxide-enhanced MR imaging. *Radiology* 1995;195:106-112
- Bellin MF, Zaim S, Auberton E, et al. Liver metastasis; safety and efficacy of detection with superparamagnetic iron oxide in MR imaging. *Radiology* 1994;193:657-663
- Quadkerk M, van den Heuvel AG, Wieloski Pa, et al. Hepatic lesions: detection with ferumoxide-enhanced T1-weighted MR imaging. *Radiology* 1997;203:449-456
- Schwarz LH, Seltzer SE, Tempany CM, et al. Superparamagnetic iron oxide hepatic MR imaging : efficacy and safety using conventional and fast spin echo pulse sequence. *J Magn Reson Imaging* 1995;5:566-570
- Van Beers BE, Lacrosse M, Jamart J, et al. Detection and segmental location of malignant hepatic tumors: comparison of ferumoxide-enhanced gradient-echo and T2-weighted spin echo MR imaging. *AJR Am J Roentgenol* 1997;168:713-717

18. Reimer P, Rummeny EJ, Daldrup HE, et al. Clinical results with Resovist: a phase 2 clinical trial. *Radiology* 1995;195:489-496
19. Jung G, Krahe T, Kugel H, et al. Detection of focal hepatic lesions : effects of superparamagnetic iron oxide on magnetic resonance imaging of the liver using T2-weighted fast spin-echo sequence and gradient- and spine-echo sequences at 1.0 Tesla. *Invest Radiol* 1998; 33:61-67
20. Hoe LV, Bosmans H, Aerts P, et al. Focal liver lesions: fast T2-weighted MR imaging with half-Fourier rapid acquisition with relaxation enhancement . *Radiology* 1996;201:817-823
21. Semelka RC, Kelekis NL, Thomasson D, Brown MA, Laub GA HASTE MR imaging ; description of technique and preliminary results in the abdomen. *J Magn Reson Imaging* 1996;201:817-823
22. Stark DD, Weissleder R, Elizondo G, et al. Superparamagnetic iron oxide: clinical application as a contrast agent for MR imaging of the liver. *Radiology* 1988;168:297-301
23. Yamamoto H, Yamashita Y, Yoshimatsu S, et al. Hepatocellular carcinoma in cirrhotic livers: detection with unenhanced and iron oxide-enhanced MR imaging. *Radiology* 1995;195:106-112
24. Marchal G, Van Hecke P, Demaerel P, et al. Detection of liver metastases with superparamagnetic iron oxide in 15 patients: Result of MR imaging at 1.5T. *AJR Am J Roentgenol* 1989;152:771-775
25. Elizondo G, Weissleder R, Stark DD, et al. Hepatic cirrhosis and hepatitis: MR imaging enhanced with superparamagnetic iron oxide. *Radiology* 1990;174:797-801
26. Clement O, Frija G, Chambon C, et al. Liver tumors in cirrhosis; experimental study with SPIO-enhanced MR imaging. *Radiology* 1991;180:31-36
27. Grandin C, Van Beer BE, Robert A, et al. Benign hepatocellular tumors: MRI after superparamagnetic iron oxide administration. *J Comput Assist Tomogr* 1995;19:412-417
28. Pockler-Schoeniger C, Koepke J, Gueckel F, et al. MRI with superparamagnetic iron oxide: Efficacy in the detection and characterization of focal hepatic lesions. *Magn Reson Imaging* 1999;17(3):383-392
29. Grangier C, Tourniaire J, Mentha G, et al. Enhancement of liver hemangioma on T1 weighted MR SE images by superparamagnetic iron oxide particles. *J Comput Assist Tomogr* 1994;18:888-896

SPIO-enhanced MR Imaging for HCC Detection in Cirrhotic Patient : Comparison of Various Techniques for Optimal Sequence Selection¹

In-Hwan Kim, M.D., Jeong-Min Lee, M.D., Hyo-Sung Kwak, M.D., Chong-Soo Kim, M.D.,
Tae Kon Kim, M.D.², Soo Tiek Lee, M.D.², Hee Chul Yu, M.D.³

¹Department of Diagnostic Radiology, Chonbuk National University Hospital

²Department of Internal Medicine, Chonbuk National University Medical School

³Department of General Surgery, Chonbuk National University Medical School

Purpose: To compare the efficacy of breathhold and non-breathhold sequences in the detection of hepatocellular carcinoma (HCC) in cirrhotic patients using superparamagnetic iron oxide (SPIO)-enhanced MR imaging, and to determine the optimal sequence combination.

Materials and Methods: By means of unenhanced and iron-oxide-enhanced MRI, 29 patients with 49 nodular HCCs were evaluated for the presence of HCC nodules. Twenty-one were male and eight were female, and their ages ranged from 38 to 71 (mean, 56) years. Eight different MR sequences were used, including four non-breath-hold sequences and four breath-hold, and images were obtained before and after the administration of SPIO particles. Non-breath-hold sequences included T2-, proton density-weighted SE, and TSE imaging, while breath-hold sequences comprised T1-weighted fast low-angle shot (T1wFLASH), half-Fourier acquisition single shot turbo spine echo (HASTE), T2-weighted fast imaging with steady-state free precession (T2*wFISP) and T2-weighted breath-hold TSE (T2wBHTSE). Image analysis involved both quantitative and qualitative analysis. The quantitative parameters calculated were signal-to-noise (S/N) ratios for livers and tumors, contrast to noise (C/N) ratios for tumors seen on precontrast and postcontrast images, and percentage of signal intensity loss (PSIL) after SPIO injection. Images were analysed qualitatively in terms of image artifacts and lesion conspicuity, and prior to calculating sensitivity, the numbers of lesions detected using various pulse sequences were counted.

Results: SPIO had a marked effect on liver S/N ratio but a minimal effect on tumor S/N ratio. PSIL was best in T2*wFISP images, while T2wSE images showed the second-best results ($p < 0.05$). Tumor-to-liver C/N values were also highest with T2*wFISP, while T2wTSE and HASTE images were next. Qualitative study showed that non-breath hold images and FISP were better than breath hold images in terms of lesion conspicuity. The latter, however, were much better than non-breath-hold images with regard to image artifacts ($p < 0.05$). Sensitivity after the injection of contrast material increased in every image sequence except T1wFLASH, and, in particular, postcontrast FISP and T2wTSE showed the best results ($p > 0.05$).

Conclusion: SPIO-enhanced MR imaging effectively detected hepatocellular carcinoma in cirrhotic livers. In terms of lesion detection and improvement of the lesion to liver C/N ratio, the FISP sequence was at least as good as non-breath-hold sequences, but if the T2 suppression effect of SPIO is to be obtained, other breath-hold sequences are not appropriate. To help lesion characterization, we suggest that T1w-FLASH and non-breath-hold T2w-TSE imaging are added to the optimal SPIO-enhanced MR imaging sequence.

Index words : Iron

Liver, MR

Liver, neoplasms

Magnetic resonance (MR), contrast enhancement

Magnetic resonance (MR), comparative studies

Address reprint requests to : Jeong-Min Lee, M.D., Department of Diagnostic Radiology, Chonbuk National University Hospital
634-18, Keumam-Dong, Chonju-shi, Chon Buk 561-712, Korea.
Tel. 82-652-250-1152 Fax. 82-652-272-0481